

Received December 27, 2020, accepted January 15, 2021, date of publication January 21, 2021, date of current version February 2, 2021.

Digital Object Identifier 10.1109/ACCESS.2021.3053298

# Micro-Doppler Radar Gait Measurement to Detect Age- and Fall Risk-Related Differences in Gait: A Simulation Study on Comparison of Deep Learning and Gait Parameter-Based Approaches

KENSHI SAHO<sup>1</sup>, (Member, IEEE), KEITARO SHIOIRI<sup>1</sup>, MASAHIRO FUJIMOTO<sup>2</sup>, AND YOSHIYUKI KOBAYASHI<sup>2</sup>

<sup>1</sup>Department of Intelligent Robotics, Toyama Prefectural University, Imizu 939-0398, Japan

<sup>2</sup>Human Augmentation Research Center, National Institute of Advanced Industrial Science and Technology, Kashiwa 277-0882, Japan

Corresponding author: Kenshi Saho (saho@pu-toyama.ac.jp)

This work was supported by the Japan Agency for Medical Research and Development (AMED) under Grant JP20dk0110041.

**ABSTRACT** This paper describes the application of micro-Doppler radar (MDR) to gait classification based on fall risk-related differences using deep learning and gait parameter-based approaches. Two classification problems were considered in this study: elderly non-fallers and multiple fallers were classified to investigate the detection of fall risk-related gait differences, and middle-aged (50s) and elderly (70s) adults were classified to detect aging-related gait differences. The MDR signal data of the participants were simulated using an open motion capture gait dataset. The classification results obtained using the deep learning and gait parameter-based approaches showed that the classification accuracy achieved using a support vector machine with the gait parameters extracted from the MDR signals was better than that resulting from the deep learning of spectrogram (time-velocity distribution) images of the MDR signals for both classification problems. The gait parameter-based approach achieved the classification rates of 79 % for faller/non-faller classification and 82 % for 50s/70s classification, whereas the corresponding accuracies were 73 % and 76 %, respectively, using the deep learning approach. These results reveal that the gait parameters extracted via MDR measurements include sufficient information on gait to detect individuals with a high risk of falls and the gait parameter-based approaches are thus effective for both classification problems.

**INDEX TERMS** Doppler radar, gait recognition, statistical analysis.

## I. INTRODUCTION

Falls often lead to morbidity and disability in the elderly. Daily gait assessment is important for evaluating the fall risks of individuals because most falls that result in physical injuries in the elderly occur while walking [1]. For this purpose, gait information that shows differences in fall risks should be effective for screening people with high fall risks. Many studies have verified the significant differences in gait between participant groups with different fall risks, such as young adults, elderly adults, and elderly adults with a history of falls [2]–[4]. In particular, elderly adults with a history of multiple falls have significant fall risks [5], [6], and the detection of such risks via the gait information is important

The associate editor coordinating the review of this manuscript and approving it for publication was Weimin Huang<sup>1</sup>.

to prevent repeated falls. Further, investigations of age-related gait changes are important to evaluate fall risks because aging is associated with slowing of gait [7], [8].

However, biomechanics researchers often have used optical motion capture (Mocap) to measure detailed gait information [2], [9]. This technique is unsuitable for daily use because of the requirements of time-consuming marker placement, numerous cameras, and a constrained environment for the participant. Accelerometry-based measurement systems, including wearable sensing techniques, have been developed to measure daily gait [3], [9]. However, participants must wear numerous acceleration sensors in these approaches. Although sensing systems using force plates or pressure mats have also been used [4], [8], their measurement areas are limited to the sensor surface and the measurable gait information is thus limited compared with that obtainable using

other sensors. To achieve simple and unconstrained gait measurement, optical remote sensing techniques such as depth sensing and camera-based analysis have been widely used [10]–[12]. However, their accuracies depend on the light conditions and clothes of the participants. In addition, none of the above techniques can measure velocity directly, which is a critical problem because one of the most important parameters in gait analysis is the walking velocity. For example, Steinert *et al.* [12] recently reported that some gait parameters such as gait speed and cadence can be measured using smartphone cameras and depth sensors to some extent. However, their accuracies are insufficient for the detailed gait measurements required in fall risk evaluation.

To resolve the above problems associated with conventional techniques, micro-Doppler radar (MDR) is a promising candidate [13]–[21]. MDR can remotely measure the velocity of whole human body parts without placing any constraints on the participant. Moreover, MDR devices are appropriately small for daily monitoring in homes, hospitals, and other such places. The effectiveness of MDR for the gait classification has been verified in rehabilitation and hospital applications [13], [14] and fall-detection systems [15]. In recent years, deep learning-based approaches involving the time-velocity diagram (spectrogram) of the MDR have achieved classification of various types of motion [16], [17] and person identification [18], [19]. Moreover, gait classification of healthy young and elderly adults based on the gait parameters related to their age- or fall risk-related gait differences was achieved in our previous work [20], [21], indicating the possibility of remotely measuring gait differences. In [21], we demonstrated the gait classification of young (aged in their 20s) and elderly (65 years and older) groups with over 80% accuracy using a support vector machine (SVM) whose feature vector was composed of the gait parameters. Thus, the measurements of detailed parameters in gait have been obtained, which will be effective for the development of a daily fall risk assessment method. However, the classification of elderly fallers was presented with quite a limited number of data in [20], and the model construction and its evaluation for practical use were not conducted. In addition, the deep learning of MDR data was not applied for such problems on the classification of participant groups that have gait differences. This state-of-the-art technique related to deep learning should be applied and compared with the conventional techniques involving gait parameter-based classification.

In this study, we demonstrated gait classification for participant groups with different ages and fall risks using MDR. The deep learning- and gait parameter-based approaches were applied and compared. We dealt with two types of gait classification problems: classification of elderly multiple fallers and non-fallers (faller classification) and gait classification in middle aged (50s) and elderly (70s) adults (50s/70s classification). The aim of the faller classification was to detect individuals with high risks of falls, and the objective of the 50s/70s classification was to detect age-related gait differences. The MDR data were simulated using the Mocap data in the AIST

Gait Database 2019 [22] because we could generate accurate MDR data for a sufficient number of participants without performing time-consuming experiments (note that recruiting participants with histories of multiple falls is difficult and time-consuming). We investigated the effectiveness of the two approaches using the MDR measurements for both gait classification problems. The contributions of this research are as follows.

- The deep learning approach was applied to faller and age classifications using MDR for the first time.
- MDR was applied to gait classification of middle-aged and elderly adults for the first time and demonstrated over 80% accuracy.
- The classification results of the deep learning and gait parameter-based approaches were compared and revealed that the gait parameter-based approach was more accurate than the deep learning approach for both classification problems.
- We demonstrated that the gait parameters extracted from spectrogram envelopes included sufficient information to classify the participant groups with different fall risks.

The remainder of this paper is organized as follows: Section II thoroughly describes the experimental participants, datasets, classification procedures, and analyses. Section III provides a detailed presentation of the classification results of the two considered approaches and comparisons with the existing published findings. Finally, Section IV highlights the main contributions of this work and topics for future research.

## II. METHODS

### A. EXPERIMENTAL PROTOCOL

This paper describes the two MDR-based gait classification problems of faller/non-faller and 50s/70s classification. The data of all participants selected for this study are included in the AIST Gait Database 2019 [22]. For the faller classification, the study participants included 28 healthy elderly adults [non-fallers: 18 men; mean age  $65.5 \pm 2.6$  years, mean height  $160.3 \pm 8.9$  cm, mean mass  $57.6 \pm 10.3$  kg] and 28 elderly adults with a history of multiple falls within one year [fallers: 12 men; mean age  $67.8 \pm 2.6$  years, mean height  $159.0 \pm 7.2$  cm, mean mass  $61.0 \pm 9.1$  kg]. The participants were aged 60 years and older, and we selected the participants so that there was no significant difference in age between the two groups, as the objective of this classification was to evaluate gait differences due to fall risk, rather than age-related gait changes. Note that participants with a history of one fall within one year were excluded in order to maximize the possibility of selecting a sample of older adults with recurrent falling problems. None of the participants had any physical disability or serious disease, such as dementia.

For the 50s/70s classification, the study participants included 35 healthy adults aged in their 50s [50s: 21 men; mean age  $53.2 \pm 2.5$  years, mean height  $166.9 \pm 7.9$  cm, mean mass  $64.0 \pm 10.2$  kg] and 35 healthy adults aged in their 70s [70s: 19 men; mean age  $72.1 \pm 1.8$  years, mean height  $159.3 \pm 7.4$  cm, mean mass  $57.8 \pm 8.9$  kg]. All participants

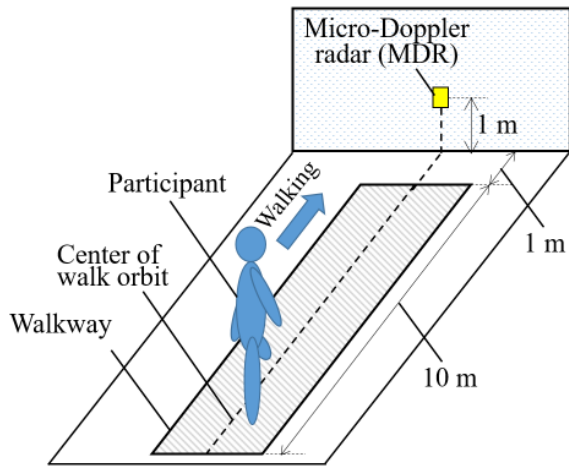


FIGURE 1. Assumed MDR measurement situation.

were healthy and did not have any physical disabilities, serious diseases, or falls within one year.

The study procedure can be summarized as follows.

1. Realistic MDR signals were generated using the Mocap data of the gait database based on a ray-tracing method [23], [24], as described in Subsection II-B.
2. Spectrograms (time-velocity distribution) of the generated MDR signals were generated using a short-time Fourier transform, as described in Subsection II-B.
3. Using the spectrograms, gait classification of the fallers/non-fallers and 50s/70s groups was conducted by utilizing the following two approaches.
  - 3-1 Deep learning approach: Spectrogram images were input into a convolutional neural network (CNN), which is a deep learning method that is known to be effective for various MDR-based motion classification problems [16]. Subsection II-C describes the details.
  - 3-2 Gait parameter-based approach: The gait parameters such as walking velocity and velocity in leg motion were extracted from the spectrograms using a method similar to that described in [21]. Then, the SVM using the extracted gait parameters was employed for classification. Subsection II-D describes the details.
4. The classification accuracies using the two approaches were evaluated and compared as explained in Subsection II-E.

## B. GENERATION OF MDR SIGNALS AND SPECTROGRAMS

In this study, simulated MDR signals generated using the AIST Gait Database 2019, which includes the Mocap data of participants walking at a comfortable pace, were employed because sufficiently accurate MDR signals can be generated as demonstrated in the conventional studies [23], [24] and recruiting a sufficient number of participants for the fallers group would have been quite time-consuming. Fig. 1 shows

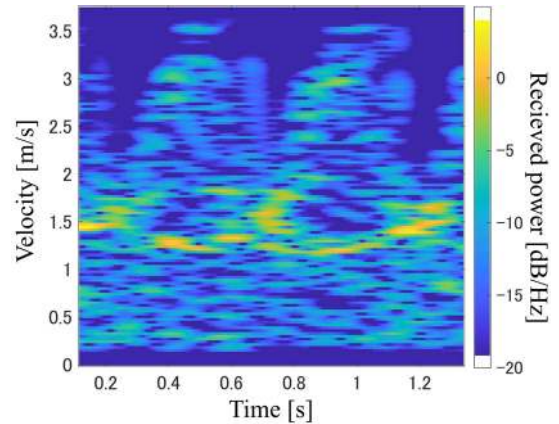


FIGURE 2. Representative spectrogram of a generated MDR signal.

the assumed MDR measurement situation. The transmitted signal was a sinusoidal wave with a frequency of 24 GHz. The received signals were calculated using the Mocap data ray-tracing method [24]. The sampling frequency of the MDR received signals was 600 Hz, which corresponds to a maximum measurement velocity of 3.75 m/s. The length of each datum was one walking cycle (approximately 1 s). For each participant, 10 data were used to generate radar data. Thus, the faller and non-faller datasets each included 280 data and the 50s and 70s datasets each included 350 data. Note that this study did not consider measurement noise and clutter to pursue the possibility of the gait classification based on fall risks.

For the gait classification using both approaches, spectrograms of the generated received signals were calculated using the short-time Fourier transform (STFT) [16]–[21]. For the STFT process, we utilized a Hamming window function with a width of 128 samples (213 ms) and an overlap length of 127 samples (these parameters were empirically optimized). The spectrogram is the map of the time-velocity-power of the received signals, where the velocity  $v$  was calculated using the frequency  $f$  and transmitting wavelength  $\lambda$  as  $v = f\lambda/2$ . Fig. 2 provides an example of the spectrogram of the data of the non-faller group. This figure shows the gait features of the body oscillations as the components with large received powers and those of the legs as relatively large velocity variations. For example, larger velocity components correspond to the forward motion of the legs and smaller velocity components correspond to the motions of the legs in contact with the floor.

## C. GAIT CLASSIFICATION USING DEEP LEARNING APPROACH

In the deep learning approach, we applied a CNN, which is a representative deep learning method for the gait classification problems similar to the MDR-based motion classification or person identification methods [16], [19]. Firstly, the spectrograms in Fig. 2 without labels, axes, and color bars were converted into JPEG images with dimensions of  $224 \times 224$

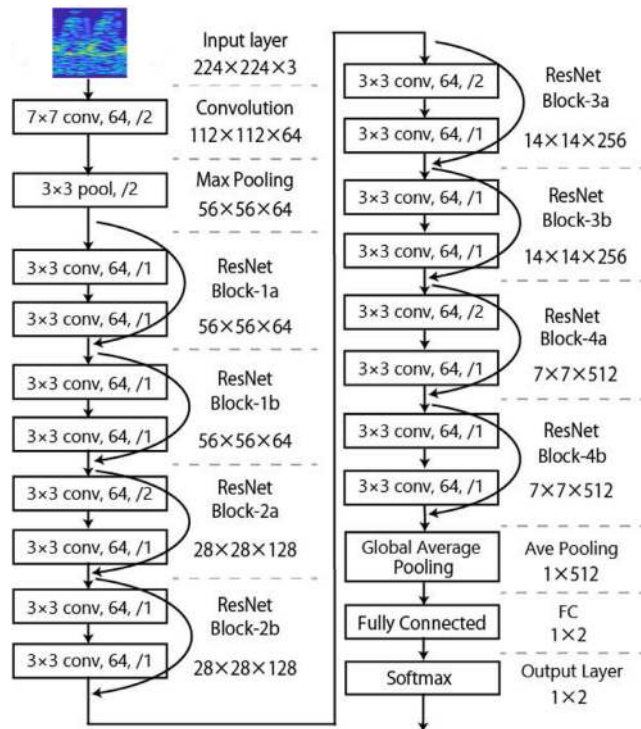


FIGURE 3. Structure of the CNN used in the deep learning approach.

pixels and RGB color. Then, the spectrogram images were input into the CNN to construct the classification models. The ResNet-18 architecture was chosen for the CNN because it was proven effective for radar-based motion recognition methods based on CNNs [16]–[19]. Subsection III-C presents classification accuracy comparisons with other representative CNNs. Fig. 3 shows the CNN with a basic ResNet-18 structure [25]. Because the input images have three color channels corresponding to RGB, the input layer is  $224 \times 224 \times 3$ . After the convolution and max pooling layers, ResNet blocks were applied. The ResNet blocks were configured in the following sequence: batch normalization (BN)–rectified linear unit (ReLU)–Convolution (Conv)–BN–ReLU–Conv. Global average pooling was performed, and a fully connected layer was then employed for class prediction using stochastic gradient descent with momentum optimization. A cross-entropy function was used as the loss function. We performed training for 200 epochs and used a batch size of 64. The learning rate was 0.01 and was decreased by multiplying it times 0.5 every 10 epochs. These hyperparameters were empirically optimized.

**D. CLASSIFICATION USING GAIT PARAMETER-BASED APPROACH**

In the gait parameter-based approach, the parameters were extracted from the spectrogram and the SVM was used for classifications, similar to the method described in [21]. Three envelopes shown in Fig. 4 were determined from the MDR spectrogram  $|S(t, \nu)|^2$  ( $t$ : time). To determine the upper and

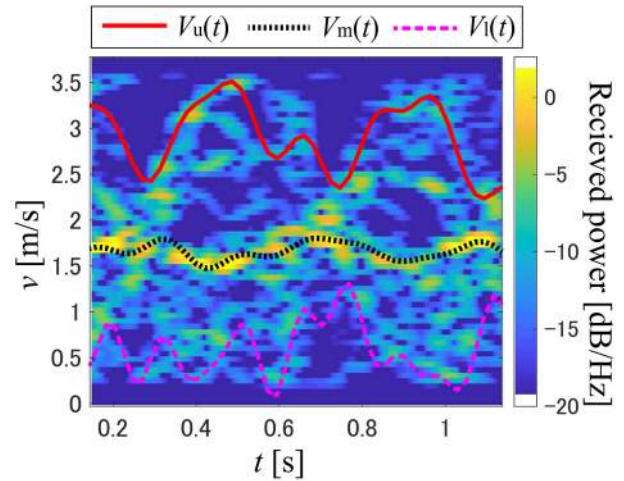


FIGURE 4. Examples of spectrogram envelope extractions.

lower envelopes, the significant peaks of  $|S(t, \nu)|^2$  for each time were identified as the components satisfying  $d|S(t, \nu)|^2/dt = 0$  and  $|S(t, \nu)|^2 > \rho \text{MAX}[|S(t, \nu)|^2]$ , where  $\text{MAX}[ \ ]$  indicates the maximum value and  $\rho < 1$  determines the threshold power for the significant peaks. In this study, we empirically set  $\rho = 0.1$ . The upper envelope  $V_u(t)$  was extracted as corresponding to the maximum  $\nu$  in the significant peaks at each  $t$  after low-pass filtering using a moving average filter with a length of 50 samples to remove effects of noise. The lower envelope  $V_l(t)$  was identified as corresponding to the minimum  $\nu$  in the significant peaks at each  $t$  using the low-pass filter, as was done for  $V_u(t)$ . Then, the mean envelope  $V_m(t) = \int \nu |S(t, \nu)|^2 d\nu / \int |S(t, \nu)|^2 d\nu$  was extracted. Using these envelopes, we calculated the 12 gait parameters defined in Table 1. Please note that some additional parameters were considered compared with our previous works [20] and [21].

The gait classifications were performed using the SVM whose feature parameters were the extracted gait parameters in Table 1. In this study, the Gaussian kernel function was chosen because it is known to be a general-purpose function for the SVM [26]. The classification hyperplane parameters were determined by utilizing a soft-margin optimization process, and the SVM parameters were optimized by performing a grid search [27].

**E. EVALUATION**

We evaluated and compared the faller and 50s/70s classification accuracies using the deep learning and gait parameter-based approaches. For the accuracy evaluations, we performed hold-out validation. In each case, the corresponding CNN and SVM were trained using 70% of the data (392 data for the faller classification and 490 data for the 50s/70s classification), and the remaining 30% of the data spectrograms were used as test data. Then, 30 trials of hold-out validations were conducted by randomly varying the training/test data split. The mean and standard deviation

**TABLE 1. List of extracted gait parameters using MDR.**

Envelope	Para.	Definition	Meaning
$V_m(t)$	$v_{m,mean}$	$E[v_m(t)]$	Mean body velocity (gait speed)
	$v_{m,std}$	$STD[v_m(t)]$	Degree of variation in body velocities
	$v_{m,max}$	$MAX[v_m(t)]$	Maximum body velocity
	$v_{m,min}$	$MIN[v_m(t)]$	Minimum body velocity
	$v_{u,mean}$	$E[v_u(t)]$	Mean leg velocity in swing phase
$V_u(t)$	$v_{u,std}$	$STD[v_u(t)]$	Degree of variation of leg velocities in swing phase
	$v_{u,max}$	$MAX[v_u(t)]$	Maximum leg velocity
	$v_{u,min}$	$MIN[v_u(t)]$	Minimum velocity leg velocity in swing phase
	$v_{l,mean}$	$E[v_l(t)]$	Mean leg velocity in stance phase
	$v_{l,std}$	$STD[v_l(t)]$	Degree of variation of leg velocity in stance phase
$V_l(t)$	$v_{l,max}$	$MAX[v_l(t)]$	Maximum leg velocity in stance phase
	$v_{l,min}$	$MIN[v_l(t)]$	Minimum leg velocity

$E[ ]$ ,  $STD[ ]$ ,  $MAX[ ]$ , and  $MIN[ ]$  indicate the mean, standard deviation, maximum value, and minimum value with respect to time  $t$  respectively.

**TABLE 2. Mean and standard deviation of classification accuracies for two classification problems using two approaches.**

	Deep learning	Gait parameter
Faller classification	$73.2 \pm 3.4 \%$	$78.9 \pm 2.7 \%$
50s/70s classification	$75.2 \pm 3.4 \%$	$81.6 \pm 1.9 \%$

**TABLE 3. Confusion matrix of faller classification.**

True \ Predicted	Fallers	Non-fallers
Fallers	$71.8 \%$ / $84.8 \%$	$28.2 \%$ / $15.2 \%$
Non-Fallers	$25.4 \%$ / $27.1 \%$	$74.6 \%$ / $72.9 \%$

Each cell indicates "the result using the deep learning approach / that using the gait parameter-based approach".

of the classification accuracy across the 30 trials were calculated.

### III. RESULTS AND DISCUSSION

#### A. CLASSIFICATION RESULTS AND COMPARISON OF TWO APPROACHES

Table 2 summarizes the means and standard deviations of the accuracies of 30 tests for the two classification problems using the two aforementioned approaches. Although the deep learning approach achieved over 70% accuracy for both problems, the gait parameter-based approach achieved better classification accuracies. Tables 3 presents confusion matrices of the faller classification results obtained using both approaches. The gait parameter-based approach accurately classified the fallers with an appropriately small false positive rate, leading this approach to be more accurate than the deep learning approach. Tables 4 presents confusion matrices of the 50s/70s classification results for both approaches. As in the faller classification, the gait parameter-based approach achieved better accuracy. In particular, the high classification accuracy for the 50s group was confirmed.

**TABLE 4. Confusion matrix of 50s/70s classification.**

True \ Predicted	50s	70s
50s	$74.4 \%$ / $86.6 \%$	$25.6 \%$ / $13.4 \%$
70s	$24.4 \%$ / $23.5 \%$	$75.6 \%$ / $76.5 \%$

Each cell indicates "the result using the deep learning approach / that using the gait parameter-based approach".

These results reveal that the spectrogram envelopes used in the gait parameter-based approach include sufficient information to classify individuals with different fall risks and that the rich information in the spectrograms used in the deep learning approach is less effective than these parameters. Although their concrete reasons cannot be revealed because the CNN mechanism is unclear, it can be predicted that mislearning due to the existence of excessively rich information in the spectrograms is one of the factors causing lower accuracy of the deep learning approach. Based on the accurate classification results obtained using the gait parameter-based approach, it can be hypothesized that the information about the main gait factor changes caused by differences in fall risk was sufficiently included in the envelopes that reflected the body and leg motions. However, in the deep learning approach, other detailed gait information, such as information about arm motion, was included in the spectrogram images and is also used for gait classification. Although some information about the age- and fall risk-related differences in gait was also included, this information was not sufficiently extracted as features and could lead to feature extraction and learning errors. Subsection III-C discusses the details of the effectiveness of the gait parameters.

#### B. COMPARISON WITH OTHER CNNs

This subsection compares the classification accuracy with those of representative CNNs other than ResNet, which were also reported to be efficient networks for motion classification using MDR spectrograms [16]: AlexNet, GoogLeNet, and VGGnet. The hyperparameters of these networks were optimized in the same manner as the ResNet-18 parameters. Table 5 presents the results and demonstrates that the CNNs other than ResNet-18 did not achieve accurate classification for the faller classification and indicates that ResNet-18 is the most effective network for the faller classification and that the residual learning in ResNet enables effective recognition of micro-motions in gait related to fall risk. On the other hand, AlexNet was effective for the 50s/70s classification same as ResNet-18. However, these results also indicate that the best accuracy of the deep learning approach is worse than that of the gait parameter-based approach for both classification problems.

#### C. DISCUSSION ON EFFECTIVENESS OF THE EXTRACTED GAIT PARAMETERS

This subsection discusses the effectiveness of the extracted parameters in the gait parameter-based approach. We investi-

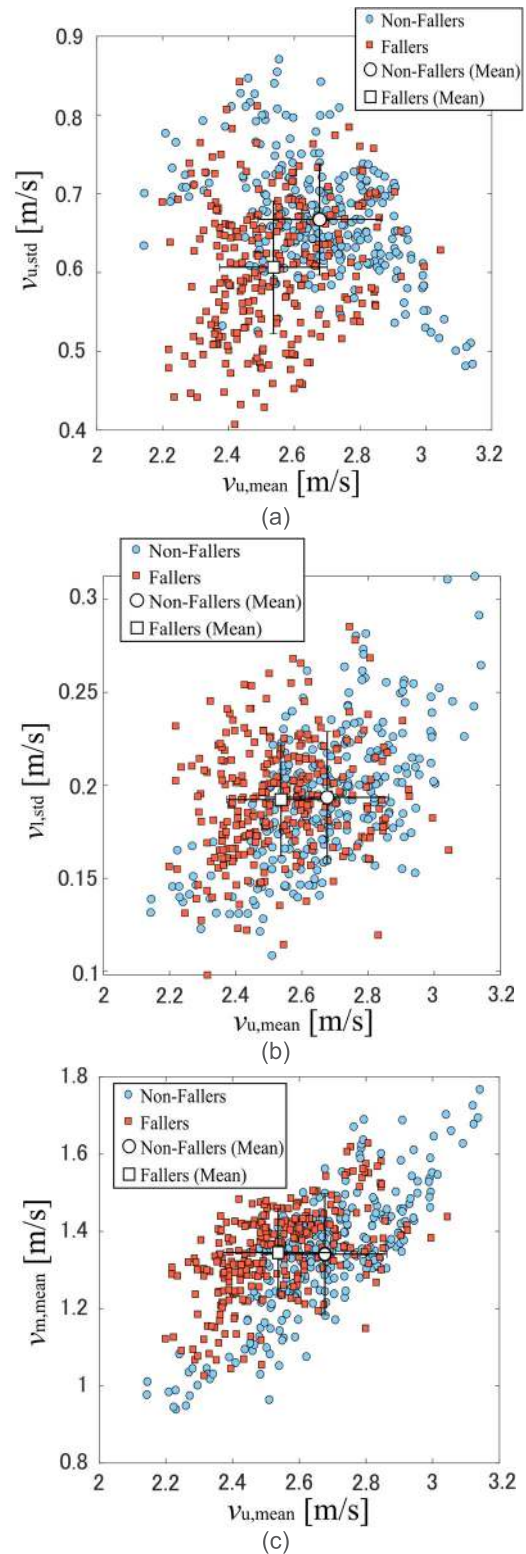
**TABLE 5. Comparison of CNN architectures.**

CNN architecture	Faller classification	50s/70s classification
AlexNet	$68.6 \pm 4.1 \%$	$75.8 \pm 2.6 \%$
GoogLeNet	$59.4 \pm 3.7 \%$	$70.5 \pm 2.7 \%$
VGGnet	$59.8 \pm 4.0 \%$	$73.8 \pm 2.6 \%$
ResNet-18	$73.2 \pm 3.4 \%$	$75.2 \pm 3.4 \%$

gated the effectiveness of the parameters extracted from each envelope. Table 6 shows the classification results obtained using the parameters of all combinations of the envelopes and SVM. The accuracy achieved using all 12 parameters extracted from the three envelopes is better than those in the other cases in which parameters of one or two envelopes were used. Thus, these three envelopes include significant information about the age- and fall risk-related differences in gait, and these results demonstrate the effectiveness and necessity of using the extracted gait parameters to classify individuals based on age- and fall risk-related differences in gait. Besides, the average time for the calculation of 12 gait parameters from the received signal was 0.917 seconds per data using a computer with a 1.7 GHz Intel Xeon bronze 3106 CPU and this computation time is adequate for real-time use.

The following discusses the details of the effectiveness of the parameters extracted from each envelope and their mechanisms. Firstly, we focus on the faller classification results, which indicate that the three spectrogram envelopes include significant information on the fall risk. For the cases in which the parameters extracted from one envelope were used, the results achieved by utilizing  $V_u(t)$  or  $V_l(t)$  were better than those obtained by using  $V_m(t)$ . These findings are consistent to our conventional results: gait differences due to fall risk is more closely related to the leg motions (corresponding to  $V_u(t)$  and  $V_l(t)$ ) than the walking speed (corresponding to  $V_m(t)$ ) [20], [21]. Further, the results for the combination of parameters extracted from  $V_u(t)$  and  $V_l(t)$  achieved highly accurate classifications compared with the cases in which the parameters extracted from each envelope were used. Fig. 5 provides example plots of the extracted gait parameters. Fig. 5(a) confirms the divergence in the plane of  $v_{u,\text{mean}}$  and  $v_{u,\text{std}}$  that are extracted from  $V_u(t)$ , and Fig. 5(b) indicates that the relationship between  $v_{u,\text{mean}}$  and  $v_{l,\text{std}}$  extracted from  $V_l(t)$  is different from that in Fig. 5(a), while preserving the clear divergence. These results reveal that the gait parameters related to both leg forward motions in swing and stance phases reflect gait differences that may reflect differences in balance ability associated with fall risks.

However, it can also be confirmed that combining the parameters extracted from  $V_m(t)$  improves the classification accuracy. In fact, the best accuracy was achieved by combining all parameters. Fig. 5(c) shows the relationship between  $v_{u,\text{mean}}$  and  $v_{m,\text{mean}}$ , which again reveals the divergence between the two groups. Thus, the gait parameters extracted from  $V_m(t)$  that reflect the body motion during walking contain fall risk information independent of the leg motions.

**FIGURE 5. Examples of plots of all participants for faller classification. (a) plots of  $v_{u,\text{mean}}$  and  $v_{u,\text{std}}$  (b)  $v_{u,\text{mean}}$  and  $v_{l,\text{std}}$  (c)  $v_{u,\text{mean}}$  and  $v_{m,\text{mean}}$ .**

That is, all gait parameters extracted from three envelopes were efficiently used for faller classification.

**TABLE 6. Classification accuracies for various combinations of gait parameters (envelopes).**

Envelopes	No. of parameters	Faller classification accuracy	50s/70s classification accuracy
$V_u(t)$	4	$71.5 \pm 3.0 \%$	$75.1 \pm 2.5 \%$
$V_m(t)$		$64.8 \pm 2.8 \%$	$57.6 \pm 3.2 \%$
$V_l(t)$		$73.6 \pm 2.6 \%$	$55.3 \pm 3.2 \%$
$V_u(t), V_m(t)$		$74.1 \pm 2.8 \%$	$76.4 \pm 3.2 \%$
$V_u(t), V_l(t)$	8	$77.7 \pm 2.5 \%$	$76.3 \pm 2.8 \%$
$V_m(t), V_l(t)$	12	$75.3 \pm 2.2 \%$	$70.0 \pm 3.0 \%$
$V_u(t), V_m(t), V_l(t)$		$78.9 \pm 2.2 \%$	$81.6 \pm 1.9 \%$

Next, we discuss the 50s/70s classification results, which are similar to the faller classification results in that the parameters extracted from all envelopes were effectively used. In the cases in which the parameters of one envelope were utilized, the results obtained using  $V_u(t)$  achieved classification and those acquired using the other two envelopes almost failed to classify 50s/70s groups. Ref. [8] reported that the differences in the stance time parameters between 50s and 70s groups were not large, whereas the differences in the step length and step width were relatively large; these characteristics explain our results. Figs. 6(a) and (b) show example plots of the parameters extracted from  $V_l(t)$  and  $V_u(t)$ , respectively. Although  $v_{l,mean}$  and  $v_{l,std}$  differ between the two groups, a clear boundary between them in this plane cannot be confirmed. In contrast, there is clear divergence between the two groups in  $v_{u,mean}$  and  $v_{u,std}$ ; thus, the parameters extracted from  $V_u(t)$  achieved accurate classification. These characteristics explain the classification results because  $V_u(t)$  reflects the step length (swing phase of gait) and  $V_l(t)$  reflects the motions in the stance phase. In addition, no significant difference in walking speed between 50s and 70s groups was reported in [7]. Thus, the parameters extracted from  $V_m(t)$  and  $V_l(t)$  were ineffective for the 50s/70s classification. However, our results demonstrated that the parameters of not only  $V_u(t)$ , but also  $V_m(t)$  and  $V_l(t)$  were effective for classification when their combinations were considered. Fig. 6(c) shows the plots of  $v_{u,std}$  and  $v_{m,mean}$ , revealing a different relationship between  $v_{u,std}$  and  $v_{m,mean}$  in comparison with that in Fig. 6(b). Furthermore, the clear divergence of the two groups is similar to that in Fig. 6(b). Thus, the combination of parameters extracted from other envelopes improved the classification accuracy. The accuracy of over 80% for the 50s/70s classification indicates that significant information related to age-related gait differences was included in the three envelopes extracted from the MDR spectrograms.

In summary, our results reveal that the motion information of the body and legs during the swing and stance phases included in the spectrogram envelopes is effective for gait classification related to both fall risk and age-related gait differences. Hence, the contributions of this study include not only accurate gait classification with our MDR-based technique, but also clarification of the effectiveness of the

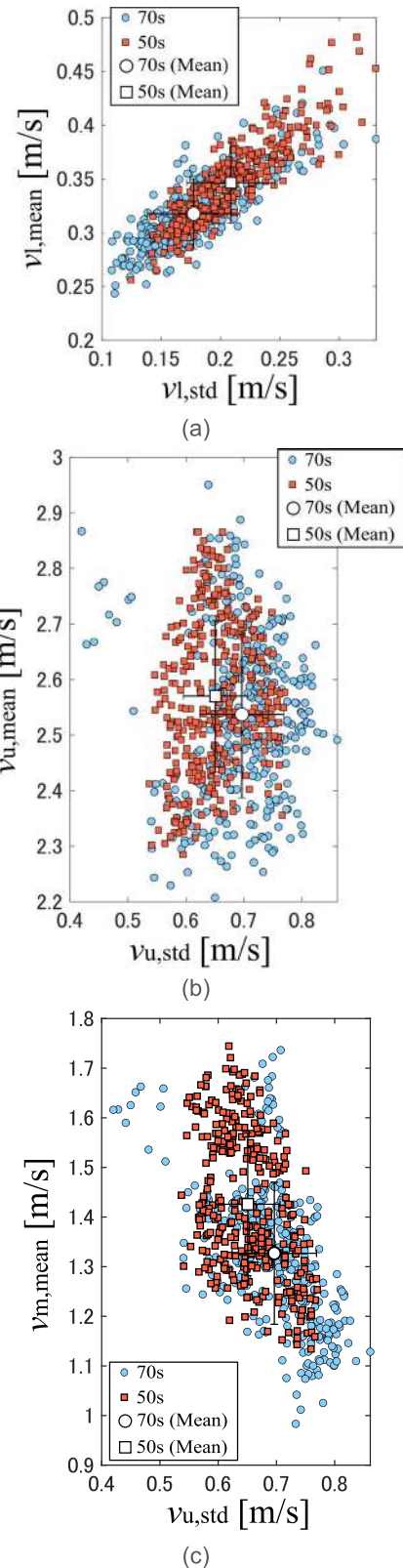


**FIGURE 6. Examples of plots of all participants for 50s/70s classification. (a) plots of  $v_{l,mean}$  and  $v_{l,std}$  (b)  $v_{u,mean}$  and  $v_{u,std}$  (c)  $v_{u,std}$  and  $v_{m,mean}$ .**

combination of the gait parameters for the detection of individuals with gait differences with respect to fall risks.

#### IV. CONCLUSION

In this study, gait classification of groups with different ages and fall risks was performed using MDR data simulated using a gait database based on deep learning and gait parameter-based approaches. The fallers/non-fallers and 50s/70s groups were classified with 78.9% and 81.6% accuracy, respectively. These results demonstrate the possibility of MDR-based detection of individuals with high risks of falls. Furthermore, although the CNN of the MDR spectrogram images achieved gait classification to some extent, the SVM whose feature vectors were gait parameters extracted via the spectrogram envelopes achieved better accuracy for both classification problems. Thus, the study results reveal that the spectrogram envelopes reflecting the leg and body motions include sufficient information related to the fall risk-related gait differences. In contrast, deep learning using spectrogram images could extract not only efficient features, but also some features that led to misclassification, other than those related to the spectrogram envelopes. Furthermore, the effectiveness of the extracted gait parameters was discussed and validated.

However, validation using actual MDR data is required as future work even though the simulated signals were accurately generated because accurate consideration of measurement noise and clutter is important to implement practical MDR systems. In addition, we performed only 50s/70s classification to investigate differences in gait due to aging. In further investigations, the gait differences of other age groups will need to be considered to find more concrete factors indicating fall risks in daily gait. Furthermore, to apply our techniques for real-life situations, experiments assuming participants walking with arbitrary directions are our important future tasks.

#### ACKNOWLEDGMENT

(Kenshi Saho and Keitaro Shioiri contributed equally to this work.)

#### REFERENCES

- [1] W. Li, T. H. M. Keegan, B. Sternfeld, S. Sidney, C. P. Quesenberry, and J. L. Kelsey, "Outdoor falls among middle-aged and older adults: A neglected public health problem," *Amer. J. Public Health*, vol. 96, no. 7, pp. 1192–1200, Jul. 2006.
- [2] M. Fujimoto and L.-S. Chou, "Sagittal plane momentum control during walking in elderly fallers," *Gait Posture*, vol. 45, pp. 121–126, Mar. 2016.
- [3] B. M. Meyer, L. J. Tulipani, R. D. Gurchiek, D. A. Allen, L. Adamowicz, D. Larie, A. J. Solomon, N. Cheney, and R. McGinnis, "Wearables and deep learning classify fall risk from gait in multiple sclerosis," *IEEE J. Biomed. Health Informat.*, early access, Sep. 18, 2020, doi: 10.1109/JBHI.2020.3025049.
- [4] A. Pradhan, U. Kuruganti, and V. Chester, "Biomechanical parameters and clinical assessment scores for identifying elderly fallers based on balance and dynamic tasks," *IEEE Access*, vol. 8, pp. 193532–193543, Oct. 2020.
- [5] A. Shumway-Cook, M. Baldwin, N. L. Polissar, and W. Gruber, "Predicting the probability for falls in community-dwelling older adults," *Phys. Therapy*, vol. 77, no. 8, pp. 812–819, Aug. 1997.
- [6] M. E. Taylor, K. Delbaere, A. S. Nikolaizak, S. R. Lord, and J. C. T. Close, "Gait parameter risk factors for falls under simple and dual task conditions in cognitively impaired older people," *Gait Posture*, vol. 37, no. 1, pp. 126–130, Jan. 2013.
- [7] D. P. LaRoche, B. L. Greenleaf, R. V. Croce, and J. A. McGaughy, "Interaction of age, cognitive function, and gait performance in 50-80-year-olds," *AGE*, vol. 36, no. 4, p. 9693, 2014.
- [8] L. K. Lau, S. L. Wee, W. J. B. Pang, K. K. Chen, K. A. Jabbar, P. L. K. Yap, J. U. Mallya, D. H. M. Ng, Q. L. L. Tan, W. T. Seah, and T. P. Ng, "Reference values of gait speed and gait spatiotemporal parameters for a South East Asian population: The Yishun study," *Clin. Interv. Aging*, vol. 15, p. 1753, 2020.
- [9] A. R. Anwary, H. Yu, A. Callaway, and M. Vassallo, "Validity and consistency of concurrent extraction of gait features using inertial measurement units and motion capture system," *IEEE Sensors J.*, vol. 21, no. 2, pp. 1625–1634, Jan. 2021, doi: 10.1109/JSEN.2020.3021501.
- [10] J. Latorre, R. Llorens, C. Colomer, and M. Alcañiz, "Reliability and comparison of Kinect-based methods for estimating spatiotemporal gait parameters of healthy and post-stroke individuals," *J. Biomech.*, vol. 72, pp. 268–273, Apr. 2018.
- [11] M. Nabila, A. I. Mohammedm, and B. J. Youssa, "Gait-based human age classification using a silhouette model," *IET Biometrics*, vol. 7, no. 2, pp. 116–124, Jun. 2018, doi: 10.1049/iet-bmt.2016.0176.
- [12] A. Steinert, I. Sattler, K. Otte, H. Röhling, S. Mansow-Model, and U. Müller-Werdan, "Using new camera-based technologies for gait analysis in older adults in comparison to the established GAITRite system," *Sensors*, vol. 20, no. 1, p. 125, 2020.
- [13] M. S. Seyfi lu, A. M. Özbayoglu, and S. Z. Gürbüz, "Deep convolutional autoencoder for radar-based classification of similar aided and unaided human activities," *IEEE Trans. Aerosp. Electron. Syst.*, vol. 54, no. 4, pp. 1709–1723, Aug. 2018.
- [14] A. K. Seifert, M. G. Amin, and A. M. Zoubir, "Toward unobtrusive in-home gait analysis based on radar micro-Doppler signatures," *IEEE Trans. Biomed. Eng.*, vol. 66, no. 9, pp. 2629–2640, Jan. 2019.
- [15] B. Jokanović and M. Amin, "Fall detection using deep learning in range-Doppler radars," *IEEE Trans. Aerosp. Electron. Syst.*, vol. 54, no. 1, pp. 180–189, Feb. 2018.
- [16] S. Z. Gurbuz and M. G. Amin, "Radar-based human-motion recognition with deep learning: Promising applications for indoor monitoring," *IEEE Signal Process. Mag.*, vol. 36, no. 4, pp. 16–28, Jul. 2019.
- [17] W. Ye and H. Chen, "Human activity classification based on micro-Doppler signatures by multiscale and multitask Fourier convolutional neural network," *IEEE Sensors J.*, vol. 20, no. 10, pp. 5473–5479, May 15, 2020.
- [18] Y. Yang, C. Hou, Y. Lang, G. Yue, Y. He, and W. Xiang, "Person identification using micro-Doppler signatures of human motions and UWB radar," *IEEE Microw. Wireless Compon. Lett.*, vol. 29, no. 5, pp. 366–368, May 2019.
- [19] K. Saho, K. Inuzuka, and K. Shioiri, "Person identification based on micro-Doppler signatures of sit-to-stand and stand-to-sit movements using a convolutional neural network," *IEEE Sensors Lett.*, vol. 4, no. 3, Mar. 2020, Art. no. 3500304.
- [20] K. Saho, M. Fujimoto, M. Masugi, and L.-S. Chou, "Gait classification of young adults, elderly non-fallers, and elderly fallers using micro-Doppler radar signals: Simulation study," *IEEE Sensors J.*, vol. 17, no. 8, pp. 2320–2321, Apr. 2017.
- [21] H. Okinaka, K. Saho, M. Fujimoto, S. Go, M. Masugi, K. Sugano, K. Uemura, and M. Matsumoto, "Gait classification of healthy young and elderly adults using micro-Doppler radar remote sensing," in *Proc. Joint 10th Int. Conf. Soft Comput. Intell. Syst. (SCIS) 19th Int. Symp. Adv. Intell. Syst. (ISIS)*, Toyama, Japan, Dec. 2018, pp. 1222–1226.
- [22] Y. Kobayashi, N. Hida, K. Nakajima, M. Fujimoto, and M. Mochimaru. (2019). *AIST Gait Database 2019*. [Online]. Available: <https://unit.aist.go.jp/harc/ExPART/GDB2019.html>
- [23] C. Karabacak, S. Z. Gurbuz, A. C. Gurbuz, M. B. Guldogan, G. Hendeby, and F. Gustafsson, "Knowledge exploitation for human micro-Doppler classification," *IEEE Geosci. Remote Sens. Lett.*, vol. 12, no. 10, pp. 2125–2129, Oct. 2015.
- [24] Y. Deep, P. Held, S. S. Ram, D. Steinhauser, A. Gupta, F. Gruson, A. Koch, and A. Roy, "Radar cross-sections of pedestrians at automotive radar frequencies using ray tracing and point scatterer modelling," *IET Radar Sonar Navig.*, vol. 14, no. 6, pp. 833–844, 2020.
- [25] K. He, X. Zhang, S. Ren, and J. Sun, "Deep residual learning for image recognition," in *Proc. IEEE Conf. Comput. Vis. Pattern Recognit. (CVPR)*, Las Vegas, NV, USA, Jun. 2016, pp. 770–778.



- [26] J. Luts, F. Ojeda, R. Van de Plas, B. De Moor, S. Van Huffel, and J. A. K. Suykens, "A tutorial on support vector machine-based methods for classification problems in chemometrics," *Analytica Chim. Acta*, vol. 665, no. 2, pp. 129–145, Apr. 2010.
- [27] C. L. Huang, M. C. Chen, and C. J. Wang, "Credit scoring with a data mining approach based on support vector machines," *Express Syst. Appl.*, vol. 33, no. 4, pp. 847–856, 2007.

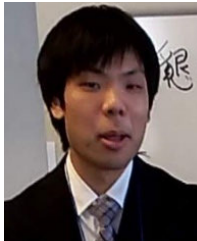


**KENSHI SAHO** (Member, IEEE) received the B.E. degree in electrical and electronic engineering, and the M.I. and Ph.D. degrees in communications and computer engineering from Kyoto University, Kyoto, Japan, in 2008, 2010, and 2013, respectively.

From 2014 to 2017, he was an Assistant Professor with the Department of Electronic and Computer Engineering, Ritsumeikan University, Japan. Since 2017, he has been a Junior Associate Professor

with the Department of Intelligent Robotics, Toyama Prefectural University, Japan. His research interests include signal processing techniques for radar imagers, sensor fusion systems for positioning and tracking, and micro-Doppler sensors.

Dr. Saho received the Best Paper Award from the ISAP2012, the Young Researcher's Award from the Radiation Science Society of Japan, in 2013, the Excellent Oral Presentation Award from the ICIAS2015, the Researcher's Award from the IEICE Intelligent Transportation Systems Technical Committee, in 2016, and the Young Scientist Award from the Funai Foundation for Information Technology, in 2017.



**KEITARO SHIOIRI** received the B.E. degree in intelligent systems design engineering from Toyama Prefectural University, Imizu, Japan, in 2019, where he is currently pursuing the M.E. degree.

His research interests include personal identification and biomechanical analysis of human movements using micro-Doppler radars based on machine learning approach.



**MASAHIRO FUJIMOTO** received the M.S. degree in mechanical engineering from Doshisha University at Kyotanabe, Kyoto, Japan, in 2006, and the Ph.D. degree in biomechanics from the University of Oregon, Eugene, OR, USA, in 2012.

From 2012 to 2014, he worked as a Postdoctoral Fellow with the University of Maryland School of Medicine, Baltimore, MD, USA. From 2014 to 2018, he was an Assistant Professor with the College of Sport and Health Science, Ritsumeikan University at Kusatsu, Japan. He is currently a Senior Researcher with the Human Augmentation Research Center, National Institute of Advanced Industrial Science and Technology (AIST), Kashiwa, Japan. His primary research interests include the biomechanics and motor control of human balance and movement, and his research has focused on fall risk assessment and fall prevention in older adults.



**YOSHIYUKI KOBAYASHI** received the Ph.D. degree from the School of Human Sciences, Waseda University, Japan.

He is currently a Team Leader with the Human Augmentation Research Center, National Institute of Advanced Industrial Science and Technology (AIST), Japan. His expertises include ergonomics, biomechanics, injury prevention, falling, gait analysis, and human modeling. He has published in a variety of peer-reviewed journals, including *Gait and Posture*, *Journal of Biomechanics*, *International Journal of Industrial Ergonomics*, and *BMC Geriatrics*.

...